Systematic Procedure for Mitigating DFIG-SSR using Phase Imbalance Compensation

DOI:
10.1109/TSTE.2021.3104719

Document Version
Accepted author manuscript

Systematic Procedure for Mitigating DFIG-SSR using Phase Imbalance Compensation

Vinay Sewdien, *Member, IEEE*, Robin Preece, *Senior Member, IEEE*, José Rueda Torres, *Senior Member, IEEE*, and Mart van der Meijden, *Member, IEEE*

***Abstract*—Replacing conventional generation by power electronics based generation changes the dynamic characteristics of the power system. This results among others in the increased susceptibility to sub synchronous oscillations (SSO). This paper proposes a systematic procedure for mitigating the interactions between a DFIG and a series compensated transmission line using the phase imbalance compensation (PIC) concept. The impact of the series and parallel PIC on the resonance behaviour of the grid is first thoroughly investigated. Then, the influence of the system strength on the capabilities of the PIC to mitigate DFIG-SSR is assessed. Based on the findings a design framework which enables the systematic assessment of the series and parallel PIC for mitigating DFIG-SSR is developed and successfully implemented in the modified IEEE 39 bus system. Comparison between both concepts reveals that the parallel PIC is better suited to mitigate DFIG-SSR. The impedance based stability analysis and detailed time domain electromagnetic transient (EMT) simulations are used to respectively screen and validate the results.**

***Index Terms*— DFIG, FACTS, MIGRATE, power electronic converters, series compensation, SSR, stability and control.**

I. Introduction

THE energy transition leads to a proliferation of power electronics interfaced generation in the power system. Under these circumstances, SSO increasingly becomes an issue [1] and can cause severe damage to power system equipment, thereby endangering operational reliability. The interaction between a doubly-fed induction generator (DFIG) and a series capacitor, first observed in Texas [2], [3], leads to such an SSO and is a form of sub synchronous resonance (SSR). Following the SSO classification of [4], this interaction is defined in the current work as DFIG-SSR.

According to [4], solutions for mitigating DFIG-SSR can be grouped into control solutions (e.g. [5]), hardware solutions (e.g. [6]) and solutions based on system level coordination (e.g. [7]). Control solutions are a cost-effective way to mitigate DFIG-SSR and tuning of the rectifier and inverter control parameters was performed for a real application in [8]. In general, controller tuning is perceived as the preferred solution to mitigate SSO, as it does not require the installation of additional capital intensive hardware. Yet, it is not always possible for two main reasons. First, controller tuning should result in a set of optimised parameters that mitigate DFIG-SSR across a wide set of operating conditions. The optimisation in [8] resulted in a set of parameters where a DFIG-SSR mode remained unstable for wind power plant dispatch levels below 25%. Second, controllers are designed to satisfy a wide range of operational and design requirements, such as fault ride through capability and power quality. Optimising the controller's response to mitigate DFIG-SSR will come at the expense of , for example, decreased power quality or a slower dynamic response of the converter. For situations when control solutions may not be preferred nor able to provide the required performance, hardware solutions can be used.

This work focuses on the PIC, which is a potential hardware solution for DFIG-SSR. The PIC concept was initially designed to mitigate SSR and can be achieved as a series or as a parallel scheme [9] as is shown in Fig. 1. In this concept a phase wide series compensation is implemented in such a way that the line impedance at the fundamental frequency is identical across all three phases, whereas the phase impedances at sub- and super synchronous frequencies are different. As such, the power system remains balanced for operation at the fundamental frequency. Only when SSR occurs, the imbalance at non-fundamental frequency will be experienced. It is exactly this characteristic that has the ability to mitigate SSR.

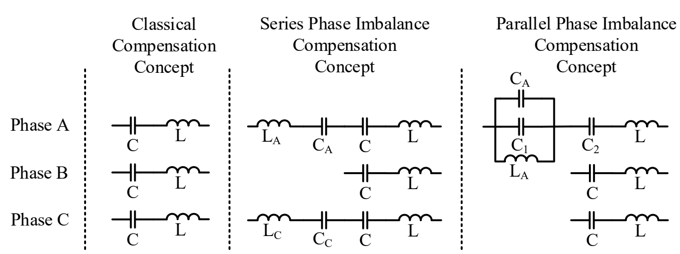

Fig. 1. Overview of the classical and series and parallel phase imbalance compensation schemes.

Existing research on PIC is limited. In [10] a case study of a real series compensated power system is presented, where the series PIC scheme was implemented in one phase to mitigate torsional SSR. The transmission line was compensated for 13%. The adequate degree of imbalance was identified using parameter search, where the objective was to find the minimum imbalance required to damp the torsional oscillations. Using

This research was carried out as part of the MIGRATE project. This project has received funding from the European Union's Horizon 2020 research and innovation programme under grant agreement No 691800. This paper reflects only the authors' views and the European Commission is not responsible for any use that may be made of the information it contains.

V. N. Sewdien, J. L. Rueda Torres and M. A. M. M. van der Meijden are with the Electrical Sustainable Energy Department, Delft Technical University, Delft, Netherlands (e-mail: vinay.sewdien@ieee.org, J.L.RuedaTorres@tudelft.nl, M.A.M.M.vanderMeijden@tudelft.nl).

R. Preece is with the School of Electrical and Electronic Engineering, The University of Manchester, UK (e-mail: robin.preece@manchester.ac.uk).

this approach, an imbalance of 0.6 was selected. It was also investigated whether splitting this imbalance over two or three phases would decrease the amount of required imbalance and it was concluded that the best damping response was obtained when the imbalance remained in one phase.

In the analysis presented in [11], PIC was deployed in one phase to mitigate torsional SSR. The transmission line was compensated for 65% and phase imbalance compensation was achieved using a single phase thyristor controlled series capacitor (TCSC). The TCSC was additionally equipped with a power oscillation damper to damp low frequency oscillations of 1.2 Hz. Time domain simulations successfully demonstrated the capability of this TCSC based PIC scheme to damp the SSR as well as the low frequency oscillation. It was additionally shown that the voltage unbalance induced in the system due to this imbalance scheme was below the recommended limits stipulated in international standards.

A similar analysis is reported in [12], where the goal of the PIC was to damp SSR and interarea oscillations of 0.78 Hz and 0.46 Hz. The PIC was introduced in one phase. Two schemes were considered for the imbalance: in scheme 1 the imbalance was achieved using a single phase static synchronous series compensator (SSSC), whereas in scheme 2 a single phase TCSC was used. Performance comparison between both schemes showed that both schemes successfully damped the oscillations, but scheme 1 had better damping capabilities.

Finally, to mitigate DFIG-SSR, the series PIC scheme was implemented in two phases of a 50% compensated transmission line in [13]. The developed imbalance scheme had a damping performance similar to supplementary damping controls of the wind farm, which resulted in completely damped oscillations within one second. Compared to other considered solutions, the imbalance scheme also provided a better transient performance during a fault and its clearing process.

To the best knowledge of the authors, other references describing the use of PIC for mitigating DFIG-SSR or any other SSO do not exist. Although the aforementioned references have studied some implementation aspects of the series and parallel PIC, research that methodically investigates the influence of the phase imbalance concept on the impedance behaviour of the grid as well as the resonance frequency of the overall system is lacking. This lack of insight is detrimental for the objective evaluation of the PIC, and consequently for its use in practical applications. In the aforementioned references the degrees of asymmetry were given without providing a holistic process on how to determine adequate degrees of asymmetry. The goal of this work is to systematically and thoroughly investigate to which extent phase imbalance compensation is able to mitigate DFIG-SSR. To this end, two main research gaps are addressed in this work. First, the influence of the series and parallel PIC schemes on DFIG-SSR will be investigated. The impact of deploying the imbalance compensation in one or two phases on the system's stability will also be assessed. Second, it will be investigated under which conditions the series and parallel PIC concept can be used to mitigate DFIG-SSR. As such, this paper makes the following three scientific contributions:

1. The impact of the series and parallel PIC on DFIG-SSR is described in terms of the phase margin and by using the impedance based stability method. The impact of the series PIC is corroborated using a mathematical analytical model and validated with EMT simulations;
2. The effectiveness of the various compensation concepts is assessed under different system strength conditions. With system strength expected to vary frequently in operational time frames [14], the insight on how the effectiveness of the concepts changes is crucial to guarantee operational reliability across a wide range of operating conditions;
3. A design methodology is proposed, which can be used to methodically assess the suitability of the series and parallel PIC schemes in mitigating DFIG-SSR across a wide range of operating conditions.

The required analysis are conducted on a small-size model and the results are validated on the modified IEEE 39 bus system.

The rest of the paper is structured as follows. Section II describes the models and methods used in this work. Section III summarises and complements the existing work on series PIC, whereas Section IV thoroughly investigates the parallel PIC. The design methodology and its application on the modified IEEE 39 bus system are presented in Section V. Section VI discusses the impact of the system strength on the various compensation schemes. Finally, the conclusions are given in Section VII.

II. Simulation Models and Analysis Methods

A. DFIG EMT Model

As DFIG-SSR is contained to a relatively small geographical area (compared to, for example, inter-area oscillations), a detail DFIG model is required for DFIG-SSR analysis. A generic detail EMT wind turbine model following the IEC standard 61400-27-1 [15] was developed in PSCAD. Semiconductor switches were modelled in detail, including the thyristors' turn on and turn off resistances, providing a realistic damping behaviour of the DFIG. An average DFIG EMT model was also developed, with the goal to investigate the need for a detailed model in the subsequent analysis. In the average model, the AC side is interfaced with voltage sources set to generate the three phase voltage references, while on the DC side a current is injected such that the power balance is preserved. A 'dummy' resistance is added in the converter of the average model, as an attempt to achieve the same level of damping provided by the switching losses in the full model. The impedance response of both models in conjunction with a series compensated transmission line (discussed in Section II B) is shown in Fig 2.

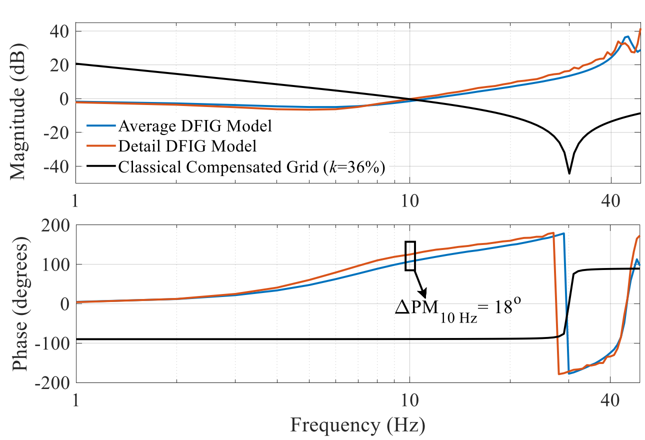

Fig. 2. DFIG-SSR assessment for classical series compensation using the average and detail DFIG EMT simulation model.

Although the resonance frequency remains 10 Hz independent of the DFIG model, the phase margin at this frequency is 18º lower when using the detailed DFIG EMT model. This means that mitigation measures designed with the detailed model need to be more stringent compared to when the average model is used. Therefore, the detailed model is used in this work.

The mechanical dynamics of the wind turbine generator were modelled using a two mass model. The classical double loop control was used as control structure of the rectifier and inverter. The implemented controls are the same as the ones used in the authors' previous work [16]. Since the controls presented in the IEC standard are meant for root mean square applications, several adaptations were implemented to make the model applicable for EMT analysis. The general behaviour and fault response of the developed model were successfully validated by a group of wind turbine generator vendors. The development of the EMT model is reported in [17]–[19] and further discussion on the model development is out of the scope of the current work.

As for fundamental frequency operation, only balanced operating conditions are considered in this work and so the DFIG is only equipped with positive sequence control. The development of negative sequence control for unbalanced operation at fundamental frequency is left as a topic for future research. Finally, as a result of the phase imbalance at sub and super synchronous frequencies, positive and negative sequence current components are developed. The damping of the negative sequence component is positive, whereas the damping of the positive sequence component is negative [10]. Therefore, only the positive sequence component is of interest.

B. Study Model

A study model is developed to investigate in detail the impact of the PIC on the positive sequence impedance behaviour of the grid. DFIG-SSR investigations reported in literature frequently use the topology of the IEEE First Benchmark Model [20] and several practical studies have used similar models, e.g. [21]–[23]. The study model in this work is depicted in Fig. 3 and a compensation degree of 36%, corresponding to a resonance frequency of 30 Hz, is imposed on the series compensated transmission line. It is worth noting that in practice the capacitance of the series capacitor would be distributed across two capacitors at both ends of the compensated transmission line. However, to better understand the fundamentals of the PIC concept, the required compensation is modelled using a single capacitor. In the scope of DFIG-SSR investigation, this approach does not influence the impedance behaviour of the transmission line and is therefore justified.

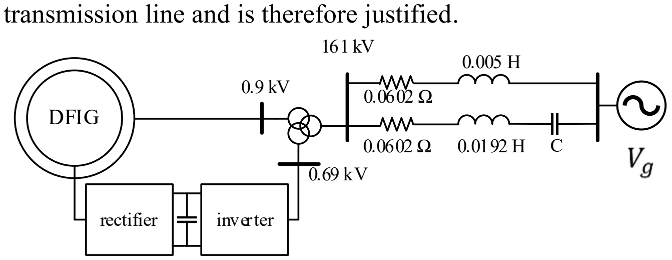

Fig. 3. Study model for PIC assessment.

C. Modified IEEE 39 Bus System

The modified IEEE 39 bus system is used in this work to validate the developed design methodology on a larger network. The EMT model of the IEEE 39 bus system is modified in three ways to accommodate DFIG-SSR analysis and is shown in Fig. 4. First, the synchronous generator at bus 9 is replaced with a DFIG wind power plant. A machine multiplier component, denoted as 'Σ', is used to scale up the DFIG and simulate a collection of machines. The aggregation of the wind turbine generators was performed following the recommendations given in [24], [25]. Second, a series capacitor with a variable degree of compensation is added to the existing transmission line between buses 9 and 29. Third, the transmission line connecting buses 26 and 29 is modified to connect buses 9 and 29, thereby creating a double circuit connection. When the uncompensated transmission line is out of service, there is a risk for DFIG-SSR.

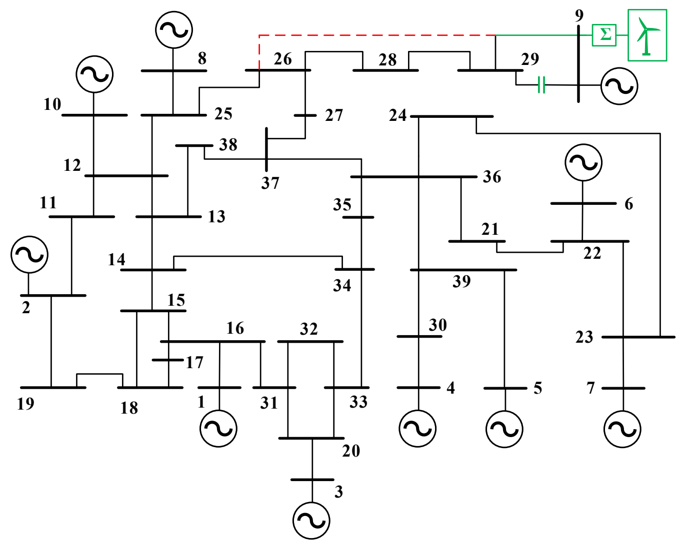

Fig. 4. Modified IEEE 39 bus system.

D. Impedance based Stability Analysis

The impedance based stability analysis [26] is used to screen for potential DFIG-SSR risks. At frequency f_r where the magnitude curves of the DFIG and the transmission grid intersect, DFIG-SSR can be potentially observed. The phase margin (PM) is a measure to quantify the system's stability, where the larger PM, the more stable the system will be. When PM at f_r is negative, DFIG-SSR will occur.

The DFIG and grid impedances are required to perform the impedance based stability analysis. These impedances are obtained using numerical simulations and the voltage perturbation method described in [27]. These numerical simulations determine three-phase quantities and for the imbalance in the grid at non-fundamental frequencies, symmetrical component analysis is used to convert phase quantities to sequence quantities.

E. Frequency Coupling

Because of nonlinearities in the converter control (e.g. the phase locked loop and rectifier current control), a frequency coupling exists at the frequency of the voltage perturbation [28]. Due to this frequency coupling, the actual PM is lower, representing a less stable system [29], [30]. The modelling of frequency coupling characteristics in a DFIG is thoroughly discussed in [31], [32]. The DFIG impedance in this work considers this frequency coupling and is obtained using the methodology described in [29].

III. Series Phase Imbalance Compensation

This Section summarises and extends the authors' previous work on the series PIC scheme [16]. Eq. (1) is the mathematical analytical model that describes the relation between the degree of asymmetry (Q), the compensation level (k) and the corresponding shift in resonance frequency (Δf_r) for the one phase series PIC and is given in the footnote[1]. See [16] for the full derivation of (1). Q is defined as C_A/C and is always positive. As such, any Q leads to an additional series capacitor and as a result the resonance frequency f_r will always increase: Δf_r is always positive and it is therefore not possible to reduce the resonance frequency using the series PIC scheme. Furthermore, for any given k, Δf_r is inversely proportional to Q. From (1) it can be observed that an imposed Δf_r in the series PIC can be achieved by modifying either k or Q. For fixed Q, modification of k (which is defined at fundamental frequency f_0) results in an altered active power transfer limit and altered Δf_r. For fixed k, modification of Q does not alter the active power transfer limit, as the impedance at f_0 should exactly be the same across the various series compensation concepts.

The positive sequence impedance responses of the DFIG and the grid for different degrees of asymmetry Q are shown in Fig. 5. It is observed that f_r is indeed inversely proportional to Q and that the two phase series PIC results in a larger Δf_r.

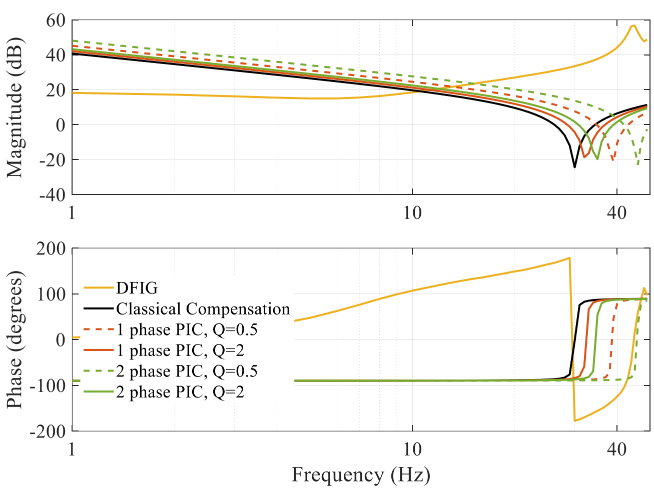

Fig. 5. Positive sequence impedance responses of DFIG and compensated transmission line. The transmission line is compensated using the classical and series PIC concepts.

Taking the positive sequence DFIG impedance and the study model into account, it is concluded that neither the one phase nor the two phase series PIC can mitigate DFIG-SSR. It was found that Δf_r is always positive, independent of Q, and that Δf_r is larger when the series PIC is implemented in two phases. As the negative resistance of the DFIG becomes more negative with an increase in f_r, it can be concluded that as long as the resonance frequency resulting from the series PIC remains within the negative resistance region of the DFIG, the stability of the system decreases even further, compared to when classical compensation is used. This decrease is more pronounced when the series PIC is deployed in two phases.

Detailed time domain simulations for $Q = 0.5$ are shown in Fig. 6. It is worth noting that the series resonances introduce a coupled super synchronous frequency component, where the frequency coupling occurs due to asymmetry in the dq control and equals $2f_0 - f_r$ [29].

The capability of the parallel PIC to mitigate DFIG-SSR is investigated next.

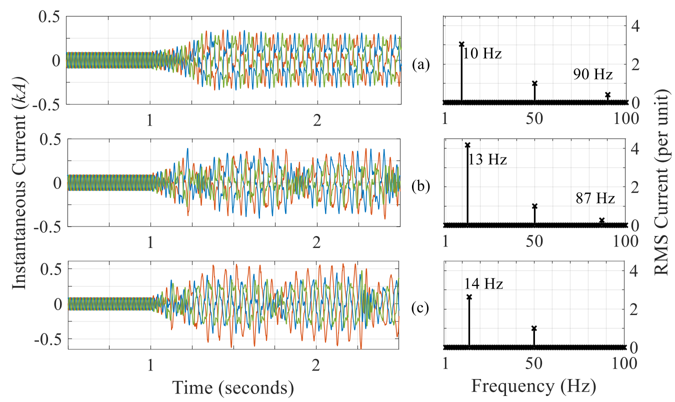

Fig. 6. Detailed time domain EMT simulations for series PIC. (a) classical compensation; (b) one phase series PIC with Q of 0.5; (c) two phase series PIC with Q of 0.5.

IV. Parallel Phase Imbalance Compensation

A. Concept Description

In line with the impedance requirement imposed on the series PIC scheme, the parallel scheme should also ensure that the impedance of all three phases at 50 Hz remains balanced and identical. Considering the parallel scheme as implemented in Fig. 1, the impedance requirement is translated to $X_A(\omega_0) = X_B(\omega_0)$. The equivalent reactance $X_{eq,1}(\omega_0)$ of the parallel resonance circuit of phase A is defined as given in (2). The total reactance $X_A(\omega_0)$ of phase A is given by (3) and the impedance requirement $X_A(\omega_0) = X_B(\omega_0)$ leads to (4). Eq. (2)-(4) are added as a footnote on the next page. Solving (4) first for L_A and then for ${\omega_0}^2$ gives (5). Substituting C_1 as defined by (6) into (5), gives (7), proofing that the impedance requirement results in the same L_A-C_A relation for the series and parallel PIC concepts. In contrast to the series PIC, each compensated phase in the parallel scheme has two degrees of freedom, namely C_1/C_2 and C_A/C_1.

---

[1]

$$Q(k,\Delta\omega_r) = \frac{(\sqrt{k{\omega_0}^2}+\Delta\omega_r)^2}{{\omega_0}^2-\left(\frac{\omega_0(\sqrt{k{\omega_0}^2}+\Delta\omega_r)}{\sqrt{k{\omega_0}^2}}\right)^2} - \frac{1}{1-\left(\frac{\sqrt{k{\omega_0}^2}+\Delta\omega_r}{\sqrt{k{\omega_0}^2}}\right)^2} \tag{1}$$

$$\frac{1}{{\omega_0}^2} = L_A C_A + L_A C_1 - L_A \frac{C_2 C}{C_2 - C} \quad (5)$$

$$C = \frac{C_1 C_2}{C_1 + C_2} \;\therefore\; C_1 = \frac{C_2 C}{C_2 - C} \quad (6)$$

$$\omega_0 = \sqrt{1/_{L_A C_A}} \quad (7)^2$$

The positive sequence impedance of phase A with classical compensation, one phase series PIC and one phase parallel PIC is shown in Fig. 7. In the classical compensation scheme k equals 36%, resulting in a series resonance at 30 Hz. The series PIC is implemented only in phase A with a Q-value (C_A/C) of 0.5. The parallel PIC is also only implemented in phase A, with C_1/C_2 and Q (C_A/C_1) of 0.5. This figure indeed illustrates that the impedance at f_0 is the same for all three compensation concepts and that the steady state behaviour at f_0 is balanced and independent of the aforementioned compensation concepts.

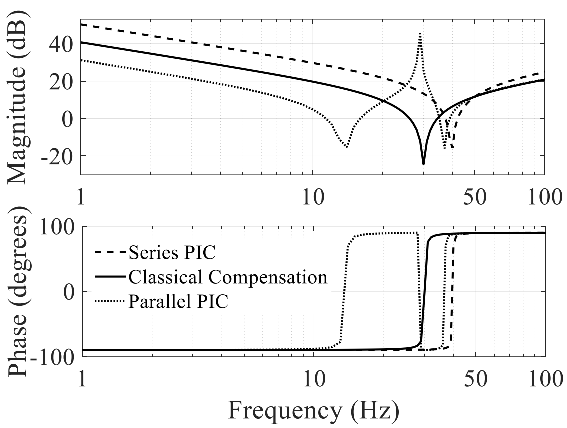

Fig. 7. Positive sequence impedance of phase A compensated using the classical and the one phase series and parallel phase imbalance concepts.

The parallel PIC concept is a combination of series and parallel resonance schemes and creates multiple resonance frequencies. In bode plots a series resonance is observed at the frequency where the magnitude curve dips and the phase curve crosses zero with a positive slope. Likewise, a parallel resonance occurs at the frequency where the magnitude curve peaks and the phase curve crosses zero with a negative slope. For the parallel PIC described above, one parallel resonance at 29 Hz and two series resonances at 14 Hz and 37 Hz are identified in the sub synchronous frequency range. The parallel PIC scheme with various degrees of asymmetry will be investigated in the following section.

B. Parallel PIC Evaluation

The positive sequence impedances of the DFIG and the transmission grid are shown in Fig. 8. The grid impedance is shown for compensation using the classical and the one phase series and parallel PIC concepts. A number of observations can be made. First, when the grid is compensated using classical compensation, the overall system has a resonance at 10 Hz, denoted as $f_{r,classical}$ in Fig. 8. Second, when series PIC is used, the resonance frequency of the overall system increases to 13 Hz, denoted as $f_{r,series\ PIC}$. The PM also reduces from -17º using classical compensation to -34º using series PIC, implying that the latter is more unstable than the former. Finally, for the parallel PIC scheme with $C_1/C_2 = C_A/C_1$= 0.5, the impedance based stability analysis identified one series resonance and one parallel resonance for the overall system. The series resonance, denoted as $f_{r,parallel\ PIC\ 1}$, occurs at 9 Hz and has a PM of -10º. The parallel resonance is denoted as $f_{r,parallel\ PIC\ 2}$ and occurs at 29 Hz. The corresponding PM is -88º.

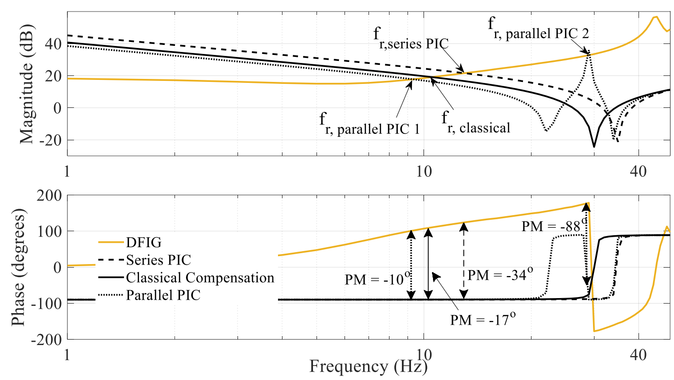

Fig. 8. Positive sequence impedance of DFIG and compensated grid.

All of the identified resonances are undamped (see Fig. 9) as their PMs are negative. The instantaneous three phase current waveforms and the accompanying harmonic spectrum for series compensation using the classical, series PIC and parallel PIC concepts are shown in Fig. 9. The resonance frequencies

---

2

$$\left.\begin{aligned} X_{C,eq}(\omega_0) &= -\frac{1}{\omega_0(C_A + C_1)} \\ X_{L,A}(\omega_0) &= \omega_0 L_A \\ X_{eq,1} &= \frac{X_{L,A} X_{C,eq}}{X_{L,A} + X_{C,eq}} \end{aligned}\right\} \Rightarrow X_{eq,1}(\omega_0) = \frac{\omega_0 L_A \frac{-1}{\omega_0(C_A + C_1)}}{\omega_0 L_A - \frac{1}{\omega_0(C_A + C_1)}} = \frac{-L_A}{\omega_0 L_A (C_A + C_1) - \frac{1}{\omega_0}} \quad (2)$$

$$X_A(\omega_0) = X_{eq,1}(\omega_0) - \frac{1}{\omega_0 C_2} + \omega_0 L = \omega_0 L - \frac{1}{\omega_0 C_2} - \frac{L_A}{\omega_0 L_A (C_A + C_1) - \frac{1}{\omega_0}} \quad (3)$$

$$\omega_0 L - \frac{1}{\omega_0 C_2} - \frac{L_A}{\omega_0 L_A (C_A + C_1) - \frac{1}{\omega_0}} = \omega_0 L - \frac{1}{\omega_0 C} \Rightarrow \frac{L_A}{L_A (C_A + C_1) - \frac{1}{{\omega_0}^2}} = \frac{C_2 - C}{C C_2} \quad (4)$$

identified using the impedance based stability analysis match the resonance frequencies observed using the detailed EMT simulations. For the parallel PIC, both the series and parallel resonances at respectively 9 and 29 Hz are observed.

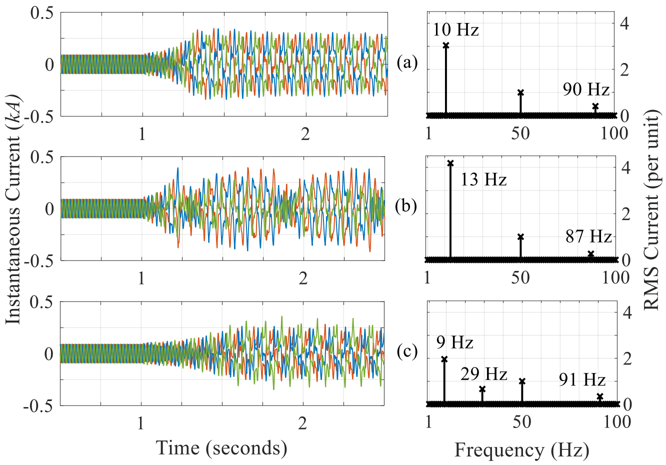

Fig. 9. Measured instantaneous current and its harmonic spectrum. (a) classical compensation; (b) one phase series PIC; (c) one phase parallel PIC.

The previous analysis focused on the performance comparison of the classical compensation and series and parallel PIC concepts. The next analysis aims at identifying the influence of the ratios C_A/C_1 and C_1/C_2 in the parallel PIC on the positive sequence impedance behaviour of the grid and how it interacts with the DFIG impedance. To this end, screening studies are performed using C_A/C_1 of 0.25, 0.5, 1 and 2 and C_1/C_2 of 0.5, 1 and 2. The results are given in Fig. 10 and show that for all the investigated cases, a series resonance of approx. 9 Hz exists in the overall system. Furthermore, the frequency of the parallel resonance is mainly influenced by C_A/C_1, whereas its magnitude is mainly affected by C_1/C_2. Apart from the series resonance at 9 Hz, the screening revealed the following three parallel resonances:

- 22 Hz for C_A/C_1 of 0.25 and C_1/C_2 of 0.5;
- 29 Hz for C_A/C_1 of 0.5 and C_1/C_2 of 0.5;
- 29 Hz for C_A/C_1 of 0.5 and C_1/C_2 of 1.0.

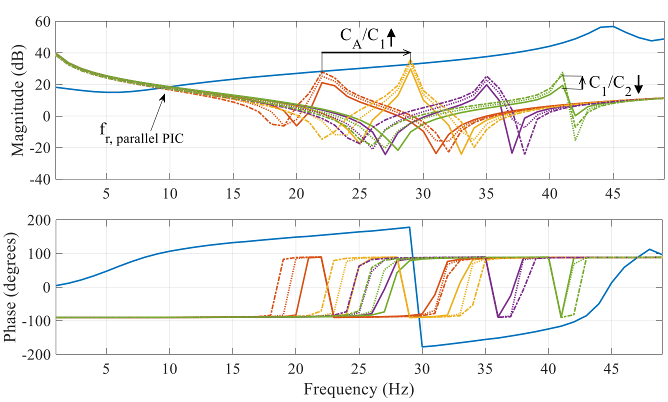

Fig. 10. DFIG-SSR screening results for different parallel PIC cases.

Fig. 11 looks more detailed into the series resonance and it is found that for all the analysed cases, the PM is between -10º and -17º, which indicates instability. The figure also shows that C_1/C_2 has a larger impact on the overall system's series resonance frequency than the C_A/C_1. As stability is only achieved when the PM is at least 0º, f_r in the overall system needs to be lower than 8 Hz. Lowering C_1/C_2 could possibly result in f_r < 8 Hz. As decreasing C_1/C_2 increases the magnitude of the parallel resonance (see Fig. 10), C_A/C_1 is fixed at 2.0 for further analysis (C_A/C_1-ratio of 2.0 has the largest difference between the positive sequence impedance magnitudes of the grid and DFIG at the parallel resonance and therefore the lowest risk for creating a parallel resonance with decreasing ratios of C_1/C_2).

Further reduction of C_1/C_2 did not result in series f_r < 8 Hz and f_r remained around 9 Hz. The PM increased from -17º under C_1/C_2-ratio 2 to approx. -6.5º under C_1/C_2-ratio 0.001. The PM for the case C_1/C_2 0.001, C_A/C_1 0.25 increases further to -4º, however, an unstable resonance appears at 23 Hz with a PM of -68º. As such, it is concluded that although the damping increases, the one phase parallel PIC is not able to sufficiently damp the 9 Hz resonance.

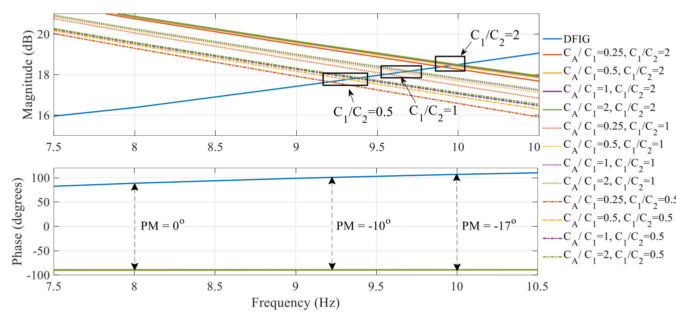

Fig. 11. Screening results for series resonance of different parallel PIC cases.

Fig. 12 provides a more detailed overview of the three parallel resonances that were identified in Fig. 10. It is found that only the resonance at 22 Hz has a positive PM (115º) and that both resonances at 29 Hz have a negative PM and are unstable. This was confirmed by EMT simulations performed for all the combinations of C_A/C_1 and C_1/C_2 shown in Fig. 10. The EMT simulations for four cases with $C_1/C_2 = 0.5$ are shown in Fig. 13. It confirms that the 22 Hz resonance is well damped (Fig. 13a) and that the resonances at 9 Hz and 29 Hz are unstable (Fig. 13b).

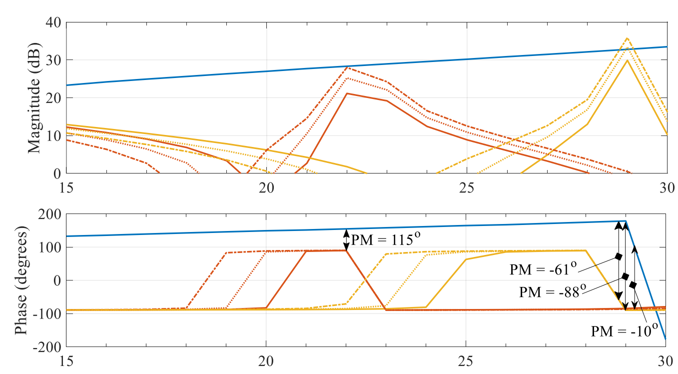

Fig. 12. Screening results for parallel resonance of parallel PIC cases.

C. Synthesis

The analysis performed so far shows that with a compensation degree of 36%, neither the series PIC nor the one phase parallel PIC were able to mitigate DFIG-SSR. The series

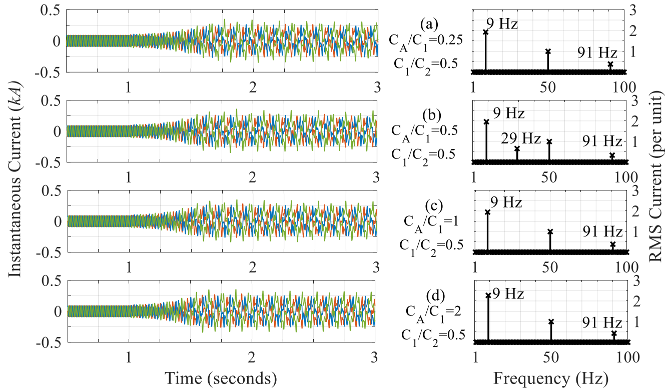

Fig. 13. Detailed time domain EMT simulations for parallel PIC with C_1/C_2-ratio of 0.5.

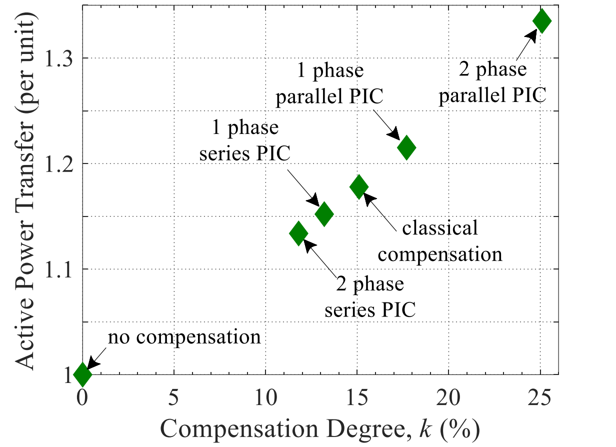

Fig. 14. Compensation degrees for different series compensation concepts leading to marginal stability of the study model.

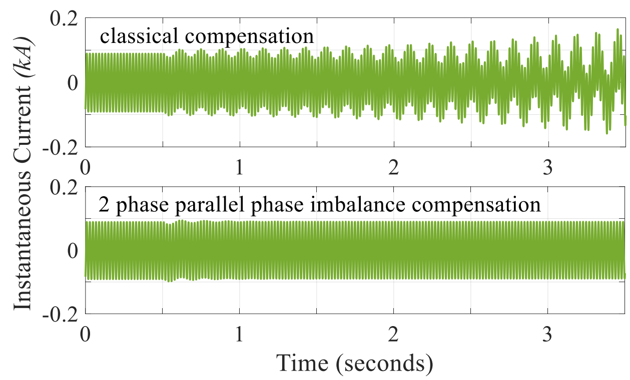

Fig. 15. Phase C instantaneous currents for 19% compensation.

PIC concept always resulted in an increase of the overall system's resonance frequency. On the other hand, the one phase parallel PIC was able to decrease the overall system's series resonance frequency to 9 Hz, however, for all the investigated cases this resonance remains unstable. Further analysis revealed that the series resonance of the overall system is only stable for f_r < 8 Hz. The parallel PIC further introduces a parallel resonance in the frequency range between 20 and 30 Hz. It was shown that depending on the ratios of C_1/C_2 and C_A/C_1 this parallel resonance can be stable.

To illustrate the influence of the various compensation concepts on DFIG-SSR, for each concept the compensation degree k resulting in a series resonance of 7 Hz is sought for. This k-value represents the marginal stability compensation degree and is identified for C_1/C_2 of 1 and C_A/C_1 of 2 in case of the parallel PIC and for C_A/C of 2 in case of the series PIC. Any compensation degree larger than the identified marginal degree will result in unstable resonances.

Fig. 14 shows for each of the series compensation concepts the compensation degree resulting in marginal stability. The active power transfer associated with the compensation degrees are indicated as well. Taking into account the positive sequence impedance profiles of the DFIG and the study model, two main conclusions can be drawn from this figure. First, compared to the classical compensation concept, the series PIC concept has a worse performance, where the two phase series PIC is less stable than the one phase series PIC. Second, the parallel PIC has a better performance than classical compensation, where the best performance is achieved using two phase parallel PIC. This essentially means that where DFIG-SSR would limit k to 15% for classical compensation, the two phase parallel PIC enables compensation up to 25%. The associated active power transfer increases from 1.17 per unit to 1.34 per unit.

With the identified marginal stability cases, it becomes clear in which cases the parallel PIC can mitigate DFIG-SSR. In Fig. 15 the EMT results are shown for a grid with 19% compensation. In line with the results from Fig. 14, the classical compensation scheme is unstable, whereas the two phase parallel PIC scheme shows a stable behaviour.

The analysis so far shows that the PIC concept has a better damping performance than the classical series compensation concept. On the other hand, there are practical considerations that need attention in the decision making to choose PIC over other methods. Three aspects are highlighted next. First, PIC always introduces additional reactors and capacitors. This requires additional space and needs to be carefully considered in the spatial planning. Second, an assessment on whether or not the rating and sizing of PIC equipment is feasible is needed. Third, expected voltage support requirements need to be considered: if voltage support is or will be needed, other solutions such as a static var compensator may be more cost-effective than PIC. The decision to use PIC should be based on thorough economic analysis as well as feasibility studies, covering the technical scarcities of today as well as the future. The next section proposes a systematic procedure to assess PIC when it is considered a possible mitigation solution.

V. Proposed Systematic Procedure

A. Development of Systematic Procedure

Based on the analyses and investigations so far, a design methodology for PIC as a DFIG-SSR mitigation solution is proposed in Fig. 16. It starts with the screening studies, which require the positive sequence DFIG and grid impedances for a wide range of topological conditions. These impedances can be obtained through numerical simulations, where frequency coupling effects need to be considered.

Using the impedance based stability analysis, the risk for DFIG-SSR is investigated next. When the magnitude plots of both impedances intersect in the sub synchronous frequency range, there is a potential risk for DFIG-SSR. If the minimum PM (considering all the grid topological conditions) at this frequency is larger than 10º, the risk is low and the analysis can be stopped. PMs lower than 10º pose a realistic risk for DFIG-SSR and would require detailed analysis. The 10º threshold is chosen based on industrial practices, but it can be any positive value at which the system operator feels confident.

When detailed analysis confirm the presence of DFIG-SSR, mitigation solutions need to be designed. At this stage, the different PIC schemes are evaluated. When the resulting PM is larger than a predefined threshold, the most effective PIC can be selected and validated using EMT simulations. This new threshold can be different from 10º and depends on the likelihood that DFIG-SSR occurs with the PIC scheme implemented and the corresponding grid topology occurring. If the PM remains lower than this threshold, PIC schemes cannot mitigate DFIG-SSR and other solutions as discussed in [4] need to be investigated. At this stage, the PIC evaluation concludes.

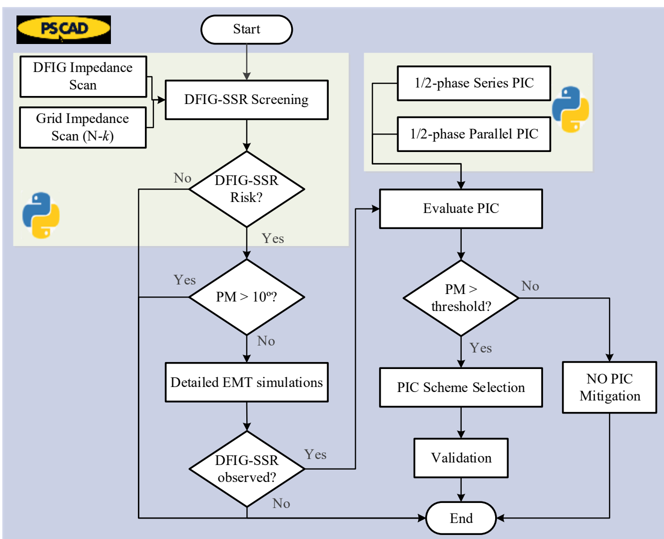

Fig. 16. DFIG-SSR mitigation using phase imbalance compensation.

B. Case Study

Next, the proposed design framework is implemented in the modified IEEE 39 bus system (Fig. 4) to mitigate DFIG-SSR. At this stage, series compensation is achieved through the classical concept. The first step consists of performing the screening studies. The positive sequence DFIG impedance is obtained using numerical simulations, and the positive sequence grid impedance is obtained for several topological conditions. Following the practical guidelines for DFIG-SSR analysis as stipulated in [33], up to N-5 conditions are considered for identifying the worst grid condition. For several of these topologies, the positive sequence impedance responses of the DFIG and the classical compensated grid intersect at approx. 12 Hz. The N-5 grid topology with lines between buses 9-29, 11-12, 13-38, 17-18 and 20-31 disconnected, results in a PM of -2.8º. This N-5 case is depicted in Fig. 17 by the black curves. The corresponding PM is below the 10º threshold, indicating high DFIG-SSR risk and is investigated in more detail. Time domain EMT simulations confirm the presence of DFIG-SSR as is shown in Fig. 18.

In the next stage, the series and parallel PIC schemes are evaluated and their capability to mitigate the observed DFIG-SSR is assessed. Fig. 17 shows the positive sequence impedance responses of the DFIG (in red) and the modified IEEE 39 bus system under classical compensation (black) and under series (in green) and parallel (in blue) PIC configurations for different degrees of asymmetry. It is confirmed again that the series PIC increases and the parallel PIC decreases f_r.

The two phase parallel PIC with $C_1/C_2 = C_A/C_1 = 0.5$ increases the PM to +28º. EMT simulations in Fig. 18 show the final validation and illustrate the effective mitigation of DFIG-SSR using these degrees of asymmetry.

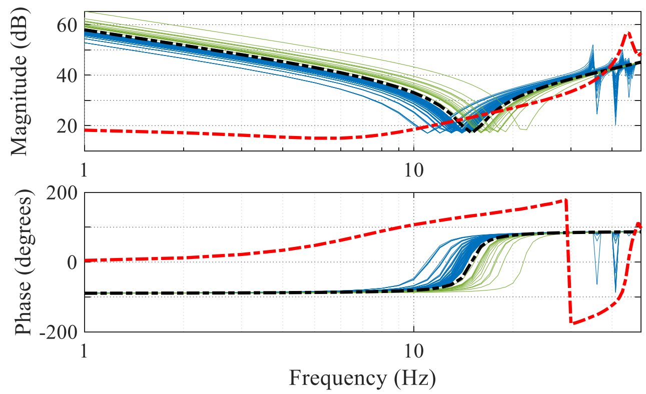

Fig. 17. Positive sequence impedance responses of DFIG (red) and the modified IEEE 39 bus system. Black curves represent the response of the N-5 grid using classical compensation. Green and blue curves represent respectively series and parallel PIC.

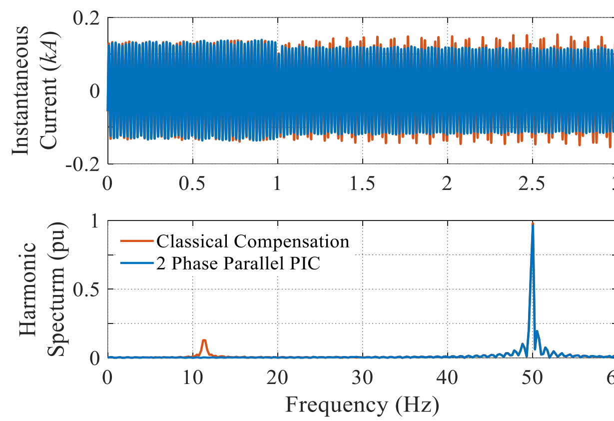

Fig. 18. Detailed time domain EMT simulations of the described N-5 topology in the modified IEEE 39 bus system.

VI. System Strength Assessment

The analysis performed so far considered a fixed system strength, where the system strength can be approximated by the equivalent inductance as seen from the PCC in the study model. The larger this inductance, the lower the system strength. For several system strength conditions, the DFIG-SSR assessment is shown in Fig. 19. The goal was to assess how the stability of the overall system changes for different system strengths. Series compensation is achieved through classical compensation with k=28% (marginal stability case for L=0.01 H).

With constant k and reducing system strength, f_r increases and the PM decreases, leading to deterioration of stability. With an equivalent inductance of 0.04 H, k should be reduced to maximum 8% in order not to observe DFIG-SSR. This k represents the compensation degree leading to marginal stability and k-values in excess of 8% will lead to DFIG-SSR.

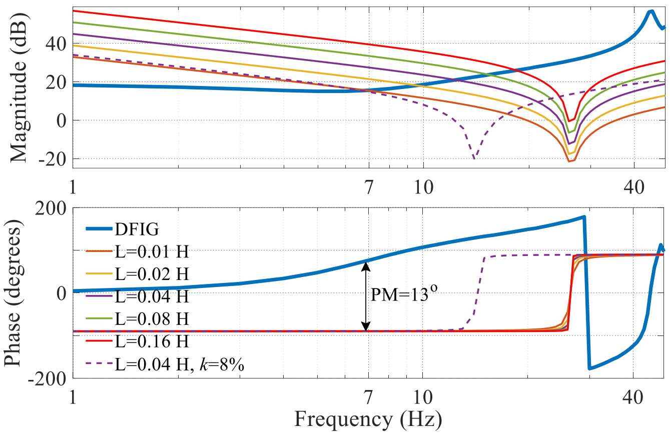

Fig. 19. DFIG-SSR screening results for different system strength conditions. Series compensation is achieved through classical compensation with k=28%.

For the system strength conditions shown in Fig. 19, the compensation degrees leading to marginal stability under the classical compensation concept as well as under the one and two phase series and parallel PIC concepts were calculated using the impedance based stability method. The results are depicted in Fig. 20 and show that independent of the series compensation concept, decreasing system strength consistently leads to decreased stability of DFIG-SSR.

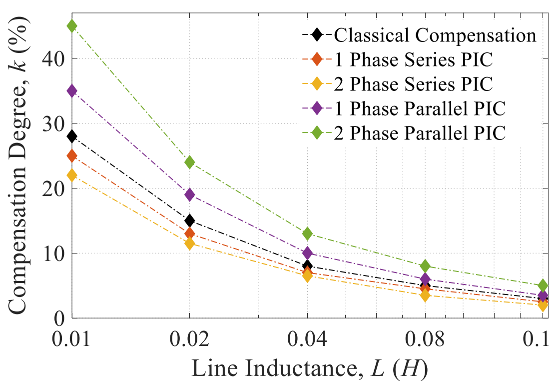

Fig. 20. Compensation degrees for different series compensation concepts leading to marginal stability under different system strength conditions.

VII. Conclusions

The goal of this work was to evaluate to which extent the phase imbalance compensation scheme, as an alternative for the classical compensation scheme, can mitigate DFIG-SSR. For the series PIC, analytical analysis and time domain simulations showed that independent of the degree of asymmetry, the corresponding resonance frequency of the overall system always increased. This increase was inversely proportional to the degree of asymmetry, and is larger when the series PIC is implemented in two phases instead of one phase. As the negative resistance of the DFIG became more negative with an increase in the resonance frequency, it was concluded that when the increased resonance frequency remains within the negative resistance region of the DFIG, the stability of the system will decrease further. Taking the positive sequence DFIG impedance and the study model into account, it was concluded that neither the one phase nor the two phase series PIC was able to mitigate DFIG-SSR.

The parallel PIC concept is a hybrid compensation concept consisting of series and parallel resonance circuits. As a result, this concept introduces multiple resonance frequencies. The conducted analysis showed that in contrast to the series PIC, the parallel PIC is able to reduce the overall system's resonance frequency, where the reduction is more pronounced when it is deployed in two phases instead of one. The resonance circuits of the parallel PIC can be tuned in such a way that the series resonance frequency occurs outside the DFIG's negative resistance region. This tuning requires special attention to ensure that also the parallel resonance remains stable.

The influence of the system strength on DFIG-SSR was also investigated. It was found that independent of the compensation concept, decreasing system strength reduces the compensation degree required for marginal stability. This essentially means that the stability margin is reduced in weak grids.

All these findings contributed to the development of a design framework, which enables the systematic assessment of the series and parallel PIC for mitigating DFIG-SSR. This framework was successfully implemented for designing a PIC scheme that is capable of mitigating DFIG-SSR in the modified IEEE 39 bus system.

Finally, the effectiveness of the impedance based stability method in accurately identifying the resonance frequencies was demonstrated.

VIII. References

[1] X. Wang and F. Blaabjerg, "Harmonic Stability in Power Electronic-Based Power Systems: Concept, Modeling, and Analysis," *IEEE Trans. Smart Grid*, vol. 10, no. 3, 2019.

[2] J. Adams, C. Carter, and S. H. Huang, "ERCOT experience with Sub-synchronous Control Interaction and proposed remediation," in *Proceedings of the IEEE Power Engineering Society Transmission and Distribution Conference*, 2012.

[3] Y. Li, L. Fan, and Z. Miao, "Replicating Real-World Wind Farm SSR Events," *IEEE Trans. Power Deliv.*, vol. 35, no. 1, 2020.

[4] V. N. Sewdien, X. Wang, J. L. Rueda Torres, and M. A. M. M. van der Meijden, "Critical Review of Mitigation Solutions for SSO in Modern Transmission Grids," *Energies*, vol. 13, no. 13, 2020.

[5] J. Shair, X. Xie, Y. Li, and V. Terzija, "Hardware-in-the-loop and field validation of a rotor-side subsynchronous damping controller for a series compensated DFIG system," *IEEE Trans. Power Deliv.*, vol. 36, no. 2, pp. 698–709, Apr. 2021.

[6] X. Zhang, X. Xie, J. Shair, H. Liu, Y. Li, and Y. Li, "A Grid-side Subsynchronous Damping Controller to Mitigate Unstable SSCI and its Hardware-in-the-loop Tests," *IEEE Trans. Sustain. Energy*, vol. 11, no. 3, pp. 1548–1558, 2020.

[7] F. Salehi, I. Brandao Machado Matsuo, A. Brahman, M. Aghazadeh Tabrizi, and W.-J. Lee, "Sub-Synchronous Control Interaction Detection: A Real-Time Application," *IEEE Trans. Power Deliv.*, vol. 35, no. 1, pp. 106–116, 2020.

[8] A. Chen, D. Xie, D. Zhang, C. Gu, and K. Wang, "PI parameter tuning of converters for sub-synchronous interactions existing in grid-connected DFIG wind turbines," *IEEE Trans. Power Electron.*, vol. 34, no. 7, pp. 6345–6355, 2019.

[9] A.-A. Edris, "Series compensation schemes reducing the potential of subsynchronous resonance," *IEEE Trans. Power Syst.*, vol. 5, no. 1, pp. 219–226, 1990.

[10] A. A. Edris, "Subsynchronous resonance countermeasure using phase imbalance," *IEEE Trans. Power Syst.*, vol. 8, no. 4, 1993.

[11] D. Rai, G. Ramakrishna, S. O. Faried, and A. A. Edris, "Enhancement of power system dynamics using a phase imbalanced series compensation scheme," *IEEE Trans. Power Syst.*, vol. 25, no. 2, pp. 966–974, 2010.

[12] D. Rai, S. O. Faried, G. Ramakrishna, and A. A. Edris, "Damping inter-area oscillations using phase imbalanced series compensation schemes," *IEEE Trans. Power Syst.*, vol. 26, no. 3, 2011.

[13] U. Karaagac, S. O. Faried, J. Mahseredjian, and A. A. Edris, "Coordinated Control of Wind Energy Conversion Systems for

Mitigating Subsynchronous Interaction in DFIG-Based Wind Farms," *IEEE Trans. Smart Grid*, vol. 5, no. 5, pp. 2440–2449, 2014.

[14] V. N. Sewdien, R. Chatterjee, M. Val Escudero, and J. van Putten, "System Operational Challenges from the Energy Transition," *CIGRE Sci. Eng.*, vol. 17, pp. 5–20, 2020.

[15] IEC, "International Standard 61400-27-1: Wind Turbines - Part 27-1: Electrical Simulation Models - Wind Turbines," Geneva, 2015.

[16] V. N. Sewdien, J. L. Rueda Torres, and M. A. M. M. van der Meijden, "Evaluation of Phase Imbalance Compensation for Mitigating DFIG-Series Capacitor Interaction," *Energies*, vol. 13, no. 17, 2020.

[17] MIGRATE, "MIGRATE Project Type 3 and Type 4 EMT Model Documentation," 2017.

[18] T. Breithaupt *et al.*, "MIGRATE Deliverable D1.2 Power System Analysis and KPIs *(confidential)*," 2018.

[19] T. Breithaupt *et al.*, "MIGRATE Deliverable D1.6 Demonstration of Mitigation Measures and Clarification of Unclear Grid Code Requirements," 2019.

[20] IEEE Subsynchronous Resonance Working Group, "First benchmark model for computer simulation of subsynchronous resonance," *IEEE Trans. Power Appar. Syst.*, vol. 96, no. 5, pp. 1565–1572, 1977.

[21] X. Xie, W. Liu, H. Liu, Y. Du, and Y. Li, "A system-wide protection against unstable SSCI in series-compensated wind power systems," *IEEE Trans. Power Deliv.*, vol. 33, no. 6, pp. 3095–3104, 2018.

[22] P. Li, L. Xiong, F. Wu, M. Ma, and J. Wang, "Sliding mode controller based on feedback linearization for damping of sub- synchronous control interaction in DFIG-based wind power plants," *Electr. Power Energy Syst.*, vol. 107, pp. 239–250, 2019.

[23] S. Zhao, N. Wang, R. Li, B. Gao, B. Shao, and S. Song, "Sub-synchronous control interaction between direct-drive PMSG-based wind farms and compensated grids," *Electr. Power Energy Syst.*, vol. 109, pp. 609–617, 2019.

[24] L. M. Fernández, C. A. García, J. R. Saenz, and F. Jurado, "Equivalent models of wind farms by using aggregated wind turbines and equivalent winds," *Energy Convers. Manag.*, vol. 50, no. 3, pp. 691–704, Mar. 2009.

[25] H. Liu and Z. Chen, "Aggregated modelling for wind farms for power system transient stability studies," in *Asia-Pacific Power and Energy Engineering Conference, APPEEC*, 2012.

[26] J. Sun, "Impedance-based stability criterion for grid-connected inverters," *IEEE Trans. Power Electron.*, vol. 26, no. 11, 2011.

[27] B. Badrzadeh, M. Sahni, Y. Zhou, D. Muthumuni, and A. Gole, "General methodology for analysis of sub-synchronous interaction," *IEEE Trans. Power Syst.*, vol. 28, no. 2, pp. 1858–1869, 2013.

[28] M. K. Bakhshizadeh *et al.*, "Couplings in Phase Domain Impedance Modeling of Grid-Connected Converters," *IEEE Trans. Power Electron.*, vol. 31, no. 10, pp. 6792–6796, Oct. 2016.

[29] W. Ren and E. Larsen, "A Refined Frequency Scan Approach to Sub-Synchronous Control Interaction (SSCI) Study of Wind Farms," *IEEE Trans. Power Syst.*, vol. 31, no. 5, pp. 3904–3912, 2016.

[30] S. Song, P. Guan, B. Liu, Y. Lu, and H. Goh, "Impedance Modeling and Stability Analysis of Grid-Interactive Converters," *Energies*, vol. 14, no. 3243, 2021.

[31] W. Liu, X. Xie, X. Zhang, and X. Li, "Frequency-Coupling Admittance Modeling of Converter-Based Wind Turbine Generators and the Control-Hardware-in-the-Loop Validation," *IEEE Trans. Energy Convers.*, vol. 35, no. 1, pp. 425–433, Mar. 2020.

[32] Y. Xu, H. Nian, T. Wang, L. Chen, and T. Zheng, "Frequency Coupling Characteristic Modeling and Stability Analysis of Doubly Fed Induction Generator," *IEEE Trans. Energy Convers.*, vol. 33, no. 3, pp. 1475–1486, 2018.

[33] J. Adams, V. A. Pappu, and A. Dixit, "Ercot experience screening for Sub-Synchronous Control Interaction in the vicinity of series capacitor banks," *IEEE Power Energy Soc. Gen. Meet.*, 2012.